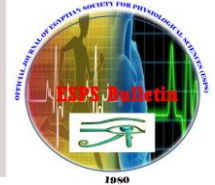




## **Bull. of Egypt. Soc. Physiol. Sci.**

(Official Journal of Egyptian Society for Physiological Sciences)

(pISSN: 1110-0842; eISSN: 2356-9514)



### **Metformin and Dapagliflozin Halt Breast Cancer Progression in Rats by Targeting microRNA-34a**

**Esraa S. Habiba<sup>1\*</sup>, Mona Hassan Fathelbab<sup>2</sup>, Marwa M. Abdelaziz<sup>3</sup>, Eman A. Allam<sup>4</sup>, Marwa Mahmoud Mady<sup>5,6</sup>, Soha Elatrebi<sup>1</sup>**

1. Clinical Pharmacology Department, Faculty of Medicine, Alexandria University, Alexandria, Egypt.
2. Medical Biochemistry Department. Faculty of Medicine, Alexandria University, Alexandria, Egypt.
3. Pathology Department, Faculty of Medicine, Alexandria University, Alexandria, Egypt.
4. Medical Physiology Department, Faculty of Medicine, Alexandria University, Alexandria, Egypt.
5. Human Anatomy and Embryology Department, Faculty of Medicine, Alexandria University, Alexandria, Egypt
6. Biomedical Science Department, Gulf Medical University, Ajman, United Arab Emirates

**Submit Date:** 21 Feb. 2025

**Accept Date:** 08 April 2025

#### **Keywords**

- Breast Cancer
- AMPK
- miRNA 34a
- Metformin
- Dapagliflozin

#### **Abstract**

**Background:** High glucose levels in breast cancer (BC) cells boost their spread and resistance to treatment by converting them into cancer stem cells. This study investigated the effects of anti-diabetic drugs metformin and dapagliflozin on tumor glucose level and the role of miRNA-34a in DMBA-induced breast cancer in rats. **Methods:** Breast cancer was induced in 24 female Wistar rats using a single oral dose of DMBA. After a breast mass of 0.5 cm<sup>3</sup> developed, the rats were divided into three groups: 8 received Metformin, 8 received Dapagliflozin, and 8 remained untreated. In contrast, 8 rats served as normal controls. Over five weeks, body weight and tumor size were monitored. At the end of the treatment, rats were euthanized, and blood and breast masses were collected to assess glucose, oxidative stress, ALDH-1, caspase 3, AMPK, and miRNA34a. Breast tissue was also evaluated histopathologically. **Results:** Rats treated with metformin showed only a partial pathological response, whereas those treated with dapagliflozin demonstrated a more improved response, with a greater reduction in tumor volume and weight loss. Moreover, dapagliflozin significantly lowered glucose levels, oxidative stress indicators, and ALDH-1 compared to metformin. It also enhanced caspase 3, AMPK, and miRNA-34a expression. **Conclusion:** Dapagliflozin and metformin combat DMBA-induced breast cancer by regulating glucose metabolism through the AMPK/miRNA 34a pathway.

## Introduction

Breast cancer (BC) is the third most prevalent malignancy worldwide and the second major cause of cancer-related death in women[1, 2]. Despite conventional approaches such as surgery, chemotherapy, hormonal treatments, and radiation, treatment failure and mortality remain on the rise globally[3]. This might be explained by the existence of breast cancer stem cells (BCSCs), which comprise a small proportion (0.1-1%) of BC tissues and are highly resistant to current therapeutic options. Aldehyde dehydrogenase-1 (ALDH-1) is a marker highly expressed by cancer stem cells, including BCSCs, along with CD44, while minimal or no expression of CD24 is observed. These features of BCSCs are thought to be responsible for the adhesion, migration, and metastasis of malignant stem cells, and consequently, they play a significant part in BC recurrence risk[4].

Dysregulation of glucose transporters (GLUTs) in cancer cells contributes to high intracellular glucose levels, promoting the transformation of malignant cells into cancer stem cells (CSCs)[5]. This transformation is explained by the "Warburg phenomenon," a biochemical process where glucose metabolism switches from oxidative phosphorylation to aerobic glycolysis with increased generation of pyruvate and lactate, even with adequate oxygen tension. Consequently, pyruvate and lactate stimulate *hypoxia-inducible factor 1-alpha* (HIF-1 $\alpha$ ) expression with further up-regulation of stemness and self-renewal factors[6]. Moreover, the aberrant activity of various signaling pathways, including Wnt/-catenin, Notch, Hedgehog, JAK-STAT, and PI3K/Akt/mTOR, contributes to the acceleration

of CSCs metastasis[7]. Hence, finding a drug targeting intracellular glucose metabolism, specifically in CSCs, may benefit patients with BC.

Sodium-glucose transporter 2 (SGLT2) is a transmembrane protein that is targeted by SGLT2 inhibitors, such as empagliflozin, canagliflozin, and dapagliflozin. These drugs are well-known oral anti-diabetic medications that reduce glucose reabsorption in the proximal renal tubule[8]. Following their approval as antidiabetic medications, there has been extensive research on their other possible therapeutic implications. SGLT2 was found to be expressed in various cancer cells, and it has been revealed that SGLT2 inhibitors may directly reduce the development of several malignancies. Different explanations have been suggested to understand the mechanisms behind this effect, such as preventing cancer cells from up-taking glucose, reducing inflammatory mediators, and enhancing AMP-activated protein kinase (AMPK) signaling[9]. On the other hand, little is known about the direct anti-tumor actions of SGLT2 inhibitors on BC cells, particularly concerning cancer metabolic reprogramming.

Metformin is the most used oral anti-diabetic agent worldwide. The metabolic effects of metformin include stimulation of the cellular uptake of glucose, an increase in hepatic glycogen synthesis, and a change in the metabolism of fatty acids through improved peripheral insulin sensitivity. These effects contribute to weight loss and stabilization of blood glucose levels without the risk of hypoglycemia[10]. Recent studies have shown a decrease in the incidence of breast, lung, pancreatic, and prostate cancer in individuals using metformin. The molecular mechanisms behind

metformin's anti-cancer effects are still unclear, even though several studies have related these effects to the activation of AMPK and the repression of the mammalian target of rapamycin (mTOR)[11, 12].

Oncogenic and tumor suppressor microRNAs (miRNAs) are different kinds of miRNAs. They are short, non-coding RNAs of around 22 nucleotides that target their complementary messenger RNA (mRNA) for post-transcriptional up-regulation or repression. One of the main miRNA families inhibiting tumor development is the miRNA-34 family, which includes three members: miRNA-34a, miRNA-34b, and miRNA-34c[13].

MiRNA-34a is highly expressed in normal tissues and is suppressed during inflammation, hypoxia, and the epithelial-mesenchymal transition (EMT)[14]. MiRNA-34a limits the ability of CSCs to self-renew, metastasize, and resist chemotherapy. Additionally, prior research indicated that miRNA34a positively correlates with AMPK and modulates tumor proliferation and apoptosis[15-17]. Notably, miRNA34a regulates the expression of GLUTs and glucose metabolism through dependent and independent interactions with the tumor suppressor p53[14].

Therefore, this study aimed to evaluate the impact of metformin and dapagliflozin on intracellular glucose in tumor cells in a rat model of DMBA-induced breast cancer by targeting AMPK and miRNA-34a.

## 2. Materials and methods

### 2.1 Ethics Statement

The Animal Ethical Committee of the Alexandria Faculty of Medicine in Egypt reviewed and agreed on the study protocol (Ethical registration no: 0306126/2023), and the principles

of the USA National Institutes of Health for the care and use of animals were followed throughout all experimental procedures[18].

### 2.2 Drugs and Chemicals

7,12-dimethylbenz[a]anthracene (DMBA) was obtained from Sigma Aldrich Chemical Co. (St. Louis, MO, USA). Metformin was procured from Minapharma Pharmaceuticals (Heliopolis, Cairo, Egypt). Dapagliflozin was purchased from AstraZeneca (Cambridge, UK). Metformin and dapagliflozin were dissolved in saline, whereas DMBA was dissolved in sesame oil.

### 2.3 Animals

The study included 32 virgin female Wistar rats, aged 55–60 days, weighing  $140 \pm 8.67$  g. They were bought from the Animal Facility of the Physiology Department at the Alexandria Faculty of Medicine, Egypt, and kept in well-ventilated plastic cages under standard environmental conditions of lighting, temperature, and humidity. Rats had free access to the regular chow diet and tap water throughout the experiment and were left for 1 week to get used to the new laboratory conditions prior to the start of the study.

### 2.4 Tumor Induction

Twenty-four rats were given a single oral dose of 80mg/kg[19] of DMBA dissolved in 1mL of sesame oil on the first day of the experiment to induce breast cancer. While 8 rats were given the same amount of sesame oil without DMBA. Six weeks later, rats were subjected to weekly palpations along both sides of the milk line until at least one mass measuring  $0.5 \text{ cm}^3$  had developed. The volume of breast mass (V) was determined using the formula  $V (\text{cm}^3) = (A \times B^2)/2$ , where the large diameter (A) and small diameter (B) are perpendicular and are expressed in centimeters (cm)[20].

## 2.5 Experimental Design and Treatment

Breast masses first appeared in rats exposed to DMBA between weeks 52 and 54. Then, the rats were divided up into four groups of eight each, and treatment was started as follows;

- Normal control group (NC): Rats received oral 0.5mL/200g body weight (BW) saline once daily for 5 weeks.
- DMBA-induced breast cancer group (DMBA): Rats received oral 0.5mL/200g BW saline once daily for 5 weeks after the development of a breast mass equals 0.5 cm<sup>3</sup>.
- Metformin-treated DMBA induced breast cancer group (DMBA+Met): Rats received oral metformin (200mg/kg)[21]once daily for 5 weeks after the development of a breast mass equals 0.5 cm<sup>3</sup>.
- Dapagliflozin-treated DMBA-induced breast cancer group (DMBA+Dapa): Rats received oral dapagliflozin (5mg/kg)[22]once daily for 5 weeks after the development of a breast mass equals 0.5 cm<sup>3</sup>.

Throughout the treatment period, the number of breast masses, their volume, and the weight of rats were all measured weekly. At the end of the 5<sup>th</sup> week of treatment (14 months post-administration of DMBA), rats were anesthetized using intramuscular xylazine (5 mg/kg) and ketamine (30 mg/kg). Blood was then drawn from the abdominal aorta into plain tubes. Afterward, breast masses were excised and divided into 2 pieces; one was kept at -80°C for later homogenization, and the other was preserved in 10% neutral buffered formalin for histological examination.

## 2.6 Samples Preparation

### 2.6.1 Blood Samples

The serum was separated after allowing blood samples to clot at room temperature for 30 min, then centrifuged for 20 min at 1500× g, and reserved at -20 °C to further assess glucose levels.

### 2.6.2 Tumor Samples

#### 2.6.2.1 Preparation of Tumor Sections

Sections were harvested from the skin and underlying mammary tissue along the mammary line. Sections were fixed in formalin. Paraffin-embedded blocks were prepared as per standard protocol. Five-micron-thick sections were prepared, stained by Hematoxylin & Eosin (H&E), and examined under light microscopy.

#### 2.6.2.2 Homogenization of Breast Tissue

The breast tissues were homogenized (100 mg tissue/ml buffer saline with protease inhibitor), and the supernatant was taken from each sample following centrifugation at 12,000x g for 15 minutes for measuring glucose levels, caspase-3, ALDH-1, AMPK, and oxidative stress markers.

#### 2.6.2.3 Determination of Glucose Level in Serum and Breast Tissue

Following directions provided by the manufacturer, the enzymatic colorimetric approach (Biomed Diagnostic, Hannover, Germany) was used to determine the level of glucose present in the serum and supernatant of the breast tissue homogenate[23]. The serum glucose level was reported as mg/dL. In contrast, the glucose level in breast tissue was normalized to the tissue protein, which was quantified using Lowry's approach and expressed as mg/mg tissue protein[24].

#### 2.6.2.4 Enzyme-linked immunoassay (ELISA) of caspase-3, ALDH-1, and AMPK

Using commercially available rat ELISA kits, the levels of AMPK (catalog No ER0730), ALDH-1 (catalog No BYEK3767), and caspase-3 (catalog No ER0143) were measured in breast tissue lysate. The samples were tested twice on a

microplate at 450 nm. Following the normalization of the ELISA findings to the total proteins of breast tissue, which were determined using Lowry's technique, the protein levels of caspase-3, ALDH-1, and AMPK in the breast tissue homogenate supernatant were expressed in ng/mg[24-27].

#### 2.6.2.5 Evaluation of Oxidative Stress Markers

The colorimetric methodology (Biodiagnostic, Cairo) was used to assess the antioxidant Superoxide dismutase (SOD) and oxidative marker Malondialdehyde (MDA) in breast tissue supernatants following the manufacturer's instructions. Thiobarbituric acid was used to determine MDA. This acid forms a reactive product when it combines with MDA in an acidic media at 95°C for 30 minutes. Meanwhile, the SOD assay relied on its capacity to prevent nitroblue tetrazolium dye from being reduced by phenazine methosulphate utilizing phosphate buffer PH 8.5, nitroblue tetrazolium, NADH, phenazine methosulphate, and an extraction reagent. Both MDA and SOD results were presented as nmol/gm tissue and U/gm tissue, respectively, after being adjusted to tissue weight[28, 29].

#### 2.6.2.6 Relative expression of miR-34a by Quantitative Real-time Polymerase Chain Reaction (RT-qPCR).

Parts of the obtained breast tissues were preserved in later (RNAlater™ Stabilization Solution, cat no AM7023), to avoid RNA breakdown, in -80 °C.

Total RNA was extracted from the breast tissue of the studied rats using the Qiagen® miRNeasy Mini Kit (catalog No. 217004, Qiagen, Germany), which combines phenol/guanidine-based lysis of samples and silica membrane-based purification of total RNA. Then, the concentration and purity of RNA were determined by NanoDrop

2000/2000c Spectrophotometer (Thermo Scientific, USA) at 260, 280, and 230 nm; ratios of A260/A280 = 1.8–2 and A260/A230 = 2–2.2 indicated highly pure RNA. The extraction was then stored at -80 °C until use.

Complementary DNA (cDNA) synthesis was performed using the miRCURY locked nucleic acid (miRCURY LNA) miRNA PCR Starter Kit. (Cat. No. 339320, Qiagen, Germany). This step was carried out in a 10 µl-reaction volume (2 µl 5x miRCURY SYBR Green RT Reaction Buffer, 1 µl 10x miRCURY RT Enzyme Mix, 5µl RNase-free water and 2 µL of each RNA (10ng/ µl) sample). Then, thermocycling was carried out as follows: reverse transcription step, 60 min at 42°C, inactivation step 5 min at 95°C, then cooling 5 min at 4°C.

**Real-time PCR** was performed using miRCURY LNA miRNA PCR Starter Kit. (Cat. No. 339320, Qiagen, Germany), including 2 LNA PCR assays of primers for miR-34a (YP00204486) as well as miR-16 (YP00205702) as an endogenous control (reference gene). Two separate PCR reactions were carried out for each sample of cDNA using miR-34a gene primers in the first reaction and miR-16 gene primers in the second reaction, each reaction contained 5µl 2x miRCURY SYBR® Green master mix, 0.5µl ROX reference dye, 1µl gene primer, 2.5µl nuclease-free water and 1µl C-DNA (20ng/reaction). Then, the Real-time cycler conditions for Applied Biosystems were carried out as follows: initial heat activation 2 min at 95°C, then 40 cycles of denaturation 10 seconds at 95°C, and combined annealing/extension 60 seconds at 56°C. In the end, a melting curve analysis was done at 60–95°C. To avoid misinterpretation, negative controls were included in all runs. Relative expression of miR-34a was calculated using  $2^{-\Delta\Delta CT}$  [30].

## 2.7 Statistical analysis of the data

Version 25.0 of IBM's Statistical Package for the Social Sciences (SPSS) software was used to analyze the data. Data normality was assessed using the Shapiro-Wilk test. The ANOVA test, followed by the post hoc Tukey's test or Kruskal-Wallis test, followed by the post hoc Dunn's multiple comparisons, was used to determine the intergroup and intragroup differences of parametric or non-parametric quantitative data, respectively. The mean  $\pm$  standard deviation (SD) was used to describe parametric quantitative data, and the median for non-parametric quantitative data. P-values less than 0.05 were regarded as statistically significant.

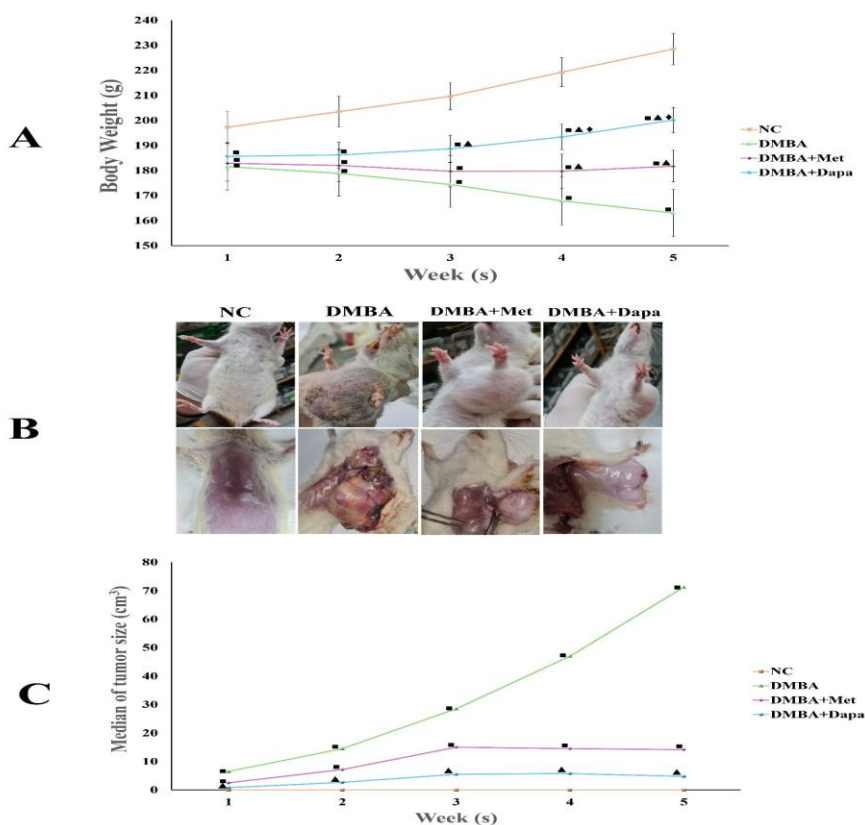
## 3. Results

### 3.1. The influence of dapagliflozin and metformin on the body weight and tumor volume of rats with DMBA-induced BC

There were notable differences in body weight amongst the groups over the five-week study duration. The DMBA-induced BC group had a significant decrease in body weight, whereas the normal control group showed a consistent gain in weight. Concurrently, weight loss was reversed by dapagliflozin and metformin treatment, with dapagliflozin having a more substantial impact than metformin ( $p < 0.05$ ; Figure 1A).

Meanwhile, the tumor sizes in the DMBA group gradually rose throughout the study duration, with a median volume of 71.25 cm<sup>3</sup> by the fifth week. On the other hand, treating rats with metformin and dapagliflozin reduced tumor growth. Dapagliflozin exhibited a more significant decrease in tumor volume than metformin, resulting in a final median tumor volume of 4.75 and 14.15 cm<sup>3</sup>, respectively ( $p < 0.05$ ; Figure 1B&C).

**Figure 1:** Influence of metformin and dapagliflozin on (A) the body weight and (B&C) tumor volume of rats with breast cancer induced by DMBA over 5 weeks. The body weight data is displayed as mean  $\pm$  SD, while the tumor volume data is displayed as the median for each group of eight rats.  $\blacksquare$   $p < 0.05$  vs. the NC group,  $\blacktriangle$   $p < 0.05$  vs the DMBA group, and  $\blacklozenge$   $p < 0.05$  vs the DMBA+Met group. NC; normal control, DMBA; Dimethylbenz[a]anthracene, Met; metformin, Dapa; dapagliflozin.

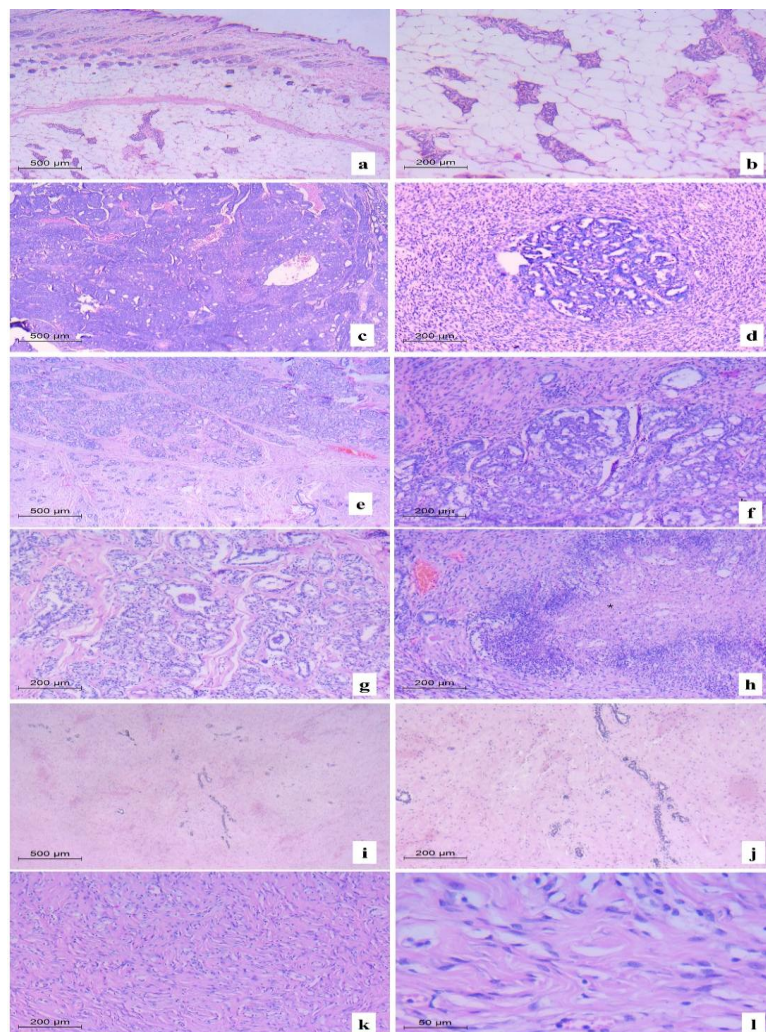


### 3.2. The influence of dapagliflozin and metformin on the breast histopathological changes induced by DMBA

The normal control shows normal mammary tissue composed of normal ducts lined by bland luminal cells resting on myoepithelial cells. The ducts are disposed against mature adipose tissue (Figure 3 a&b). On the other hand, the DMBA breast cancer group revealed invasive cancer composed of invasive ductal structures, some of which are fused into cribriform masses lined by malignant cells having pleomorphic hyperchromatic nuclei. Invasive single cells are noted. The stroma is also desmoplastic (Figure 2 c&d).

In contrast, the metformin-treated group shows a partial pathological response with viable tumor cells adjacent to normal ducts without invasion. Some tumor cells show vacuolated cytoplasm and hyperchromatic pleomorphic nuclei. Additionally, areas of necrosis rimmed by lymphocytes are noticed adjacent to the tumor (Figure 2 e-h). Meanwhile, the dapagliflozin-treated group reveals a complete pathological response with no viable tumor cells and dense fibrotic stroma. The tumor bed shows fibroblasts, histiocytes, and lymphocytes disposed against dense collagenous stroma (Figure 2 i-l).

**Figure 2:** Photomicrographs of breast tissue of rats with breast cancer induced by DMBA. **(a&b):** normal control group. a: The normal control group shows intact skin and normal underlying mammary tissue. b: Mammary tissue in the normal control group comprises normal ducts disposed against mature adipose tissue. **(c&d):** DMBA group. c: shows invasive cancer composed of invasive ductal structures, some fused into cribriform masses. d: invasive cancer comprises individual invasive cells and fused ductal structures lined by hyperchromatic pleomorphic cells. The stroma is dense desmoplastic. **(e-h):** Metformin-treated BC group. e: shows viable tumor (upper) adjacent to normal ducts (lower). f: tumor comprises fused malignant ductal structures lined by hyperchromatic pleomorphic nuclei. g: some tumor cells show vacuolated cytoplasm. h: necrotic areas (asterisk) rimmed by lymphocytes are seen adjacent to the viable tumor(left). **(i-l):** Metformin-treated BC group. i: low power showing no viable tumor tissue. j: higher power showing normal ductal structures disposed against fibrotic stroma. k: complete pathological response in the tumor bed with fibrotic areas only and no viable tumor cells. l: higher power showing dense collagenous stroma with artifactual clefts, bland fibroblasts, histiocytes, and lymphocytes. [H&E].



### 3.3. The influence of dapagliflozin and metformin on serum and breast tissue glucose levels of rats with DMBA-induced BC

Serum glucose levels showed no notable differences between the groups. However, breast tissue glucose levels were considerably higher in

the BC group than in the NC group ( $p < 0.05$ ). Additionally, metformin and dapagliflozin reduced glucose levels in breast tissue, with dapagliflozin demonstrating a much more significant reduction than metformin ( $p < 0.05$ ; Figure 3).

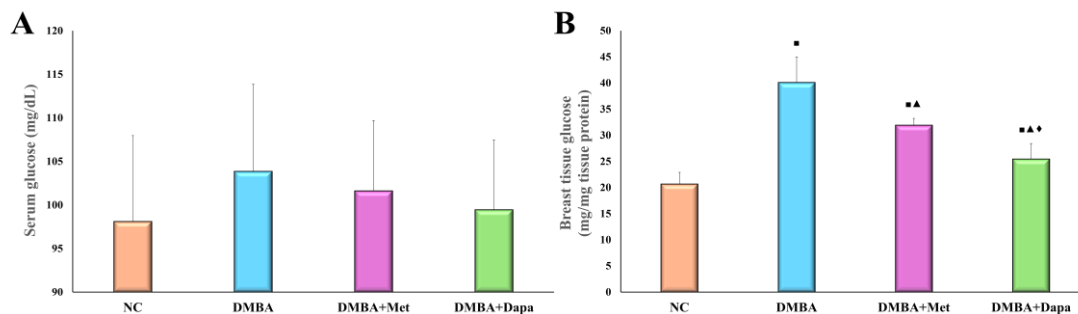


**Figure 3:** Influence of metformin and dapagliflozin on (A) serum and (B) breast tissue glucose levels of rats with breast cancer induced by DMBA. The data is displayed as mean  $\pm$  SD for each group of eight rats.  $\blacksquare p < 0.05$  vs. the NC group,  $\blacktriangle p < 0.05$  vs the DMBA group, and  $\blacklozenge p < 0.05$  vs the DMBA+Met group. NC; normal control, DMBA; Dimethylbenz[a]anthracene, Met; metformin, Dapa; dapagliflozin.

### 3.4. The influence of dapagliflozin and metformin on oxidative stress markers of rats with DMBA-induced BC

The BC group showed significantly higher MDA levels and lower SOD activity, which are indicative of increased oxidative stress and compromised breast tissue antioxidant capability.

These alterations were reversed by metformin and dapagliflozin treatments, with dapagliflozin exhibiting a stronger antioxidant capacity than metformin ( $p < 0.05$ ; Figure 4).

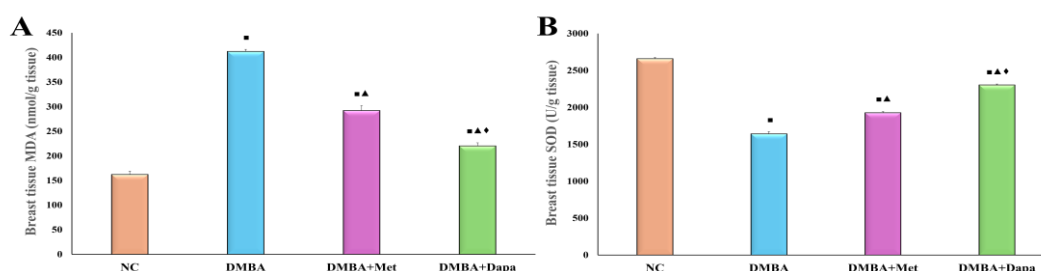


**Figure 4:** Influence of metformin and dapagliflozin on (A) breast tissue MDA levels (B) breast tissue SOD activity of rats with breast cancer induced by DMBA. The data is displayed as mean  $\pm$  SD for each group of eight rats.  $\blacksquare p < 0.05$  vs. the NC group,  $\blacktriangle p < 0.05$  vs the DMBA group, and  $\blacklozenge p < 0.05$  vs the DMBA+Met group. NC; normal control, DMBA; Dimethylbenz[a]anthracene, Met; metformin, Dapa; dapagliflozin, MDA; malonaldehyde, SOD; superoxide dismutase.

### 3.5. The influence of dapagliflozin and metformin on apoptotic and stem cell markers of rats with DMBA-induced BC

An indicator of apoptosis, caspase-3, was markedly lower in the BC group. Meanwhile, dapagliflozin caused its level to rise significantly, surpassing metformin ( $p < 0.05$ ). Aldehyde

dehydrogenase-1 (ALDH-1), a marker linked to CSCs, was, on the other hand, considerably increased in the untreated DMBA group and decreased by both treatments ( $p < 0.05$ ; Figure 5),

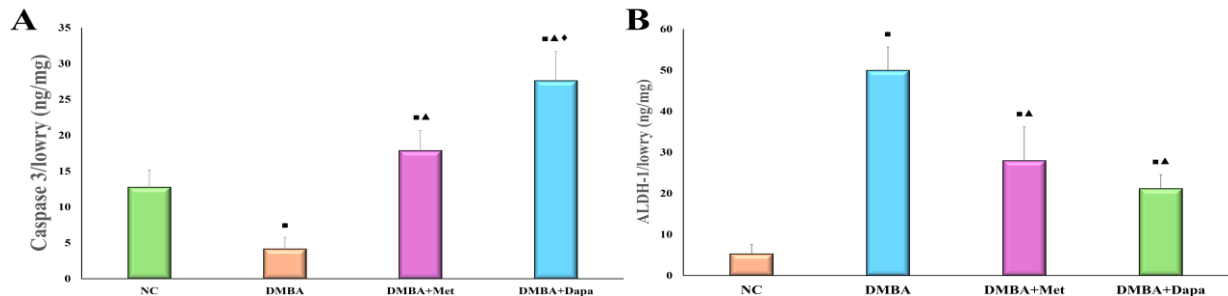


**Figure 5:** Influence of metformin and dapagliflozin on (A) caspase 3 and (B) aldehyde dehydrogenase (ALDH-1) levels in breast tissues of rats with breast cancer induced by DMBA. The data is displayed as mean  $\pm$  SD for each group of eight rats.  $\blacksquare$   $p < 0.05$  vs. the NC group,  $\blacktriangle$   $p < 0.05$  vs the DMBA group, and  $\blacklozenge$   $p < 0.05$  vs the DMBA+Met group. NC; normal control, DMBA; Dimethylbenz[a]anthracene, Met; metformin, Dapa; dapagliflozin.

### 3.6. The influence of dapagliflozin and metformin on the expression of AMPK and miRNA-34a of rats with DMBA-induced BC

AMPK levels were significantly reduced in the BC group but were restored by both treatments. Dapagliflozin treatment resulted in higher AMPK levels than metformin ( $p < 0.05$ ). Relative expression of miRNA-34a was also significantly

downregulated in the BC group, with both treatments restoring its expression. Dapagliflozin treatment showed the highest expression levels, approaching those of the NC group ( $p < 0.05$ ; Figure 6).

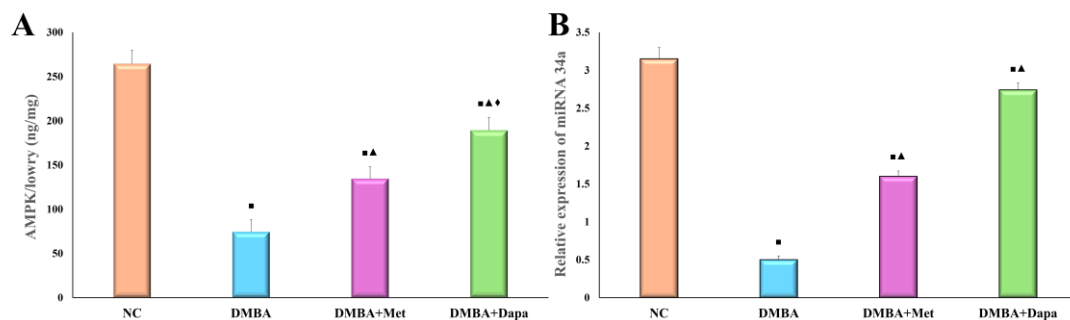


**Figure 6:** Influence of metformin and dapagliflozin on (A) AMPK levels and (B) the relative expression of miRNA 34a in breast tissues of rats with breast cancer induced by DMBA. The data is displayed as mean  $\pm$  SD for each group of eight rats.  $\blacksquare$   $p < 0.05$  vs. the NC group,  $\blacktriangle$   $p < 0.05$  vs the DMBA group, and  $\blacklozenge$   $p < 0.05$  vs the DMBA+Met group. NC; normal control, DMBA; Dimethylbenz[a]anthracene, Met; metformin, Dapa; dapagliflozin.

## 4. Discussion

Despite the availability of different therapeutic options for BC management, many patients face treatment failure and/or recurrence, leading to significant morbidity and mortality.

Also, the high risk of adverse drug reactions and elevated costs can force BC victims to discontinue their treatment. Furthermore, the ability of breast cancer stem cells (BCSCs) to self-renew and differentiate into diverse cell types raises the risk

of resistance to chemotherapy, accelerating the growth and dissemination of BC. Hence, finding safe, effective, and affordable alternatives is crucial[31, 32].

Through glycolysis, glucose provides the required energy for tumor metabolism, growth, proliferation, angiogenesis, and dissemination. The elevated intracellular glucose has been reported to be related to the increased expression of GLUTs in stem and non-stem tumor cells[31, 33]. Accordingly, in this study, we used anti-diabetic drugs that modulate AMPK, namely metformin and dapagliflozin, to target intracellular glucose in tumor cells and identify the possible implication of miRNA-34a in DMBA-induced BC in rats.

DMBA is the most utilized, highly potent polycyclic aromatic hydrocarbon for inducing BC in rats that mimics human BC by causing DNA damage[34]. The breast alveolar buds of the female Wistar rats are highly differentiated by 55 to 60 days, increasing their susceptibility to carcinogenic chemicals. After receiving a single dose of DMBA (80 mg/kg) between the ages of 55 and 60 days, 100% of rats in the current study developed masses along the milk line. These masses proliferated throughout the 5-week study period and were associated with progressive weight loss[35, 36]. The latter may be caused by an imbalance between food intake and abnormal protein metabolism, leading to a loss of strength and muscle mass[37].

Meanwhile, histopathological examination revealed that the untreated rats exhibited invasive carcinoma characterized by malignant cells with pleomorphic hyperchromatic nuclei and desmoplastic stroma, consistent with other studies' morphological and histological alterations[1, 38,

39]. Increased oxidative stress in this study, as evidenced by elevated MDA levels and decreased SOD activity, may account for these changes. This imbalance in tissue redox status is triggered by the active carcinogenic metabolite of DMBA, which raises oxidative stress by generating reactive oxygen species (ROS). These ROS peroxidize polyunsaturated fatty acids in cell membranes, leading to the production of MDA. Further, elevated MDA promotes breast cancer development by upregulating oncogenic genes and downregulating tumor suppressor genes through the formation of DNA adducts[40, 41].

Additionally, the notable reduction in AMPK, a cellular energy sensor, and caspase 3, an apoptosis marker, alongside the elevation of aldehyde dehydrogenase-1 (ALDH-1), a marker linked to CSCs in the DMBA-exposed group, explains the tumors' progressive growth during the study duration and increased tissue glucose levels. These changes are supported by previous studies[42-44], which indicated that increased oxidative stress leads to the upregulation of the PI3K/Akt/mTOR pathway, resulting in the inhibition of AMPK in tumor cells. This inhibition is associated with the suppression of the p53-p21 pathway, which contributes to the ongoing process of growth and proliferation of tumors. This process is characterized by enhanced activity of anabolic pathways, a reduction in the activity of intrinsic and extrinsic apoptotic pathways, as well as the maintenance and self-renewal of BCSCs[45-52].

Koppenol et al.[53] explained the increased activity of anabolic pathways by the increased cancer cells' glucose uptake and alterations in glucose metabolism, contributing to their resistance against commonly used

chemotherapeutic drugs. These alterations direct glucose preferentially towards lactate production rather than oxidative mitochondrial metabolism despite an increased glucose influx in tumor cells. The elevated synthesis of lactate and other intermediate metabolites from glucose promotes cell proliferation and tumor growth by activating various anabolic pathways that supply the essential elements necessary for new cell formation, proliferation, and metastasis, in contrast to glucose metabolism in normal cells, which is primarily crucial for energy production[54].

Hence, the treatment of rats with a breast mass of 0.5 cm<sup>3</sup> with oral antidiabetic drugs, metformin or dapagliflozin, led to a substantial reduction in tumor growth throughout the 5-week treatment period compared to the untreated rats with breast cancer. The antitumor effect of these medications is consistent with epidemiological, *in vitro*, and *in vivo* studies that demonstrated a correlation between their administration and a lower incidence of BC in diabetic patients, as well as a reduction in tumor growth when any of these medications were used to treat cell lines or animals with BC[10, 55-58]. However, the chemotherapeutic effect of metformin and dapagliflozin in an *in vivo* rat model of DMBA-induced BC needs further investigation and comparison between the effects of both drugs.

The notable *in vivo* reduction in glucose levels in tumor cells by administering oral metformin and dapagliflozin may elucidate the diminished tumor growth by hindering the synthesis of lactate and other intermediates essential for tumor proliferation and growth. Other *in vitro* studies have confirmed this finding, indicating that inhibiting glycolysis or

withdrawing glucose inhibits anabolic processes, which in turn reduces tumor development and carcinogenesis[59]. The withdrawal of glucose might be explained by the downregulation of the GLUTs and SGLTs transporters, which are essential for glucose uptake into tumor cells[60].

Metformin and dapagliflozin are oral antidiabetic drugs that control blood glucose levels by different mechanisms. Inhibition of hepatic gluconeogenesis, increased hepatic glycogen synthesis, and alteration of fatty acid metabolism through enhanced peripheral insulin sensitivity and antagonism of glucagon actions are among the metabolic effects of metformin[10]. In contrast, dapagliflozin inhibits SGLT2 to enhance urine glucose excretion while decreasing glucose reabsorption in the proximal renal tubule[8]. Nonetheless, the molecular mechanisms underlying their anti-cancer actions remain uncertain despite several studies linking these actions to the downregulation of glucose transporters. SGLT2 inhibitors have been shown to reduce the expression of GLUTs and SGLTs transporters, whereas metformin primarily inhibits the GLUT1 transporter[61, 62]. These observations substantiate the significant drop in glucose levels in tumor cells of rats given dapagliflozin compared to metformin.

In the current study, glucose deprivation led to decreased proliferation of both tumor cells and BCSCs and restored the normal histological features of breast tissue. This is demonstrated by a significant reduction in ALDH-1 enzyme levels, increased caspase 3 levels, and histopathological examination of breast masses of rats treated with either metformin or dapagliflozin. The considerable rise in AMPK and miRNA34a

expression in this study may help to explain these findings.

Prior research demonstrated that dapagliflozin and metformin can raise AMPK, but the effects of the two medications have not been compared[63]. Metformin raises AMPK by inhibiting the mitochondrial transport chain, which lowers mitochondrial ATP synthesis, raises the AMP/ATP ratio, and further activates AMPK. Additionally, it inhibits the lysosomal proton pump vATPase, which promotes AMPK to be phosphorylated and activated by calcium/calmodulin-dependent protein kinase kinase 2 (CaMKK2)[64, 65]. Meanwhile, dapagliflozin, by its noteworthy inhibition of glucose transporters[62], reduces glucose uptake by cells, resulting in caloric restriction and the activation of AMPK. It further interferes with the mitochondrial transport chain, resulting in a further reduction of ATP and the activation of AMPK[66, 67]. Through downstream suppression of mTOR and p53 and Nrf2 activation, increased AMPK shifts the cell into an energy-conserving state, mediating apoptotic and antioxidant effects and inhibiting anabolic pathways[15, 63, 68].

The anticancer effects of AMPK in our study were mediated by upregulating miRNA34a expression. Previous studies have shown that miRNA34a has a positive relationship with AMPK and regulates tumor growth and apoptosis[15-17]. In ovarian cancer cells, miRNA34a upregulation triggered the apoptotic pathway and reduced tumor cell proliferation, invasion, and migration[69]. MiRNA34a has also been shown to inhibit cancer stemness in prostatic cancer by specifically targeting the WNT and Notch signaling pathways[70]. In contrast, an in vitro study of

human breast cancer tissues revealed that miR-34a expression was downregulated in comparison to normal breast tissues and that this expression had a negative correlation with the clinicopathological characteristics of breast cancer[71]. MiRNA34a activation may be p53-dependent, but it can also be p53-independent and linked to the activation of antioxidant genes[15, 72].

Although both drugs activate AMPK, the notable anticancer effects of dapagliflozin in contrast to metformin, may be attributed to the modulatory effects of SGLT2 inhibitors on inflammatory pathways, ferroptosis, calmodulin receptors, and lipid metabolism, which have been linked to the development and progression of breast cancer in studies utilizing canagliflozin and empagliflozin[73-76].

Overall, metformin and dapagliflozin demonstrated in this study anticancer properties against DMBA-induced BC, with dapagliflozin showing more pronounced effects. They promoted apoptosis, attenuated the growth of stem and non-stem tumor cells, and regulated glucose metabolism through their stimulatory effect on the AMPK/miRNA 34a pathway. These results point to a possible new molecular mechanism underlying the anticancer effects of metformin and dapagliflozin. However, further in vivo animal studies are recommended to evaluate the anticancer effects of various doses of these drugs on different molecular and metabolic pathways, both individually and in combination with each other, as well as alongside other chemotherapeutic drugs.

**Funding:** The authors did not receive any financial support for this work.

**Disclosure statement:** The authors report there are no competing interests to declare

**Data availability statement:** The data that supports the findings of this study are available on request from the corresponding author.

**Author contributions:** E.S.H. and S.E. were responsible for the conceptualization and design of the study. E.S.H., E.A.A., and S.E. conducted experimental procedures. M.H.F. carried out the biochemical analyses. While M.M.A. conducted the histopathological analysis and E.S.H. performed the statistical analysis. E.S.H., M.H.F., M.M.A., E.A.A., M.M.M., and S.E. wrote the manuscript draft and reviewed it.

## References

- Sahin K, Tuzcu M, Sahin N, Akdemir F, Ozercan I, Bayraktar S, et al.** Inhibitory effects of combination of lycopene and genistein on 7,12-dimethyl benz(a)anthracene-induced breast cancer in rats. *Nutr Cancer*. 2011;63(8):1279-1286. doi: 10.1080/01635581.2011.606955
- Torre LA, Islami F, Siegel RL, Ward EM, Jemal A.** Global Cancer in Women: Burden and Trends. *Cancer Epidemiol Biomarkers Prev*. 2017;26(4):444-457. doi: 10.1158/1055-9965.epi-16-0858
- Costa E, Ferreira-Gonçalves T, Cardoso M, Coelho JMP, Gaspar MM, Faisca P, et al.** A Step Forward in Breast Cancer Research: From a Natural-Like Experimental Model to a Preliminary Photothermal Approach. *Int J Mol Sci*. 2020;21(24):9681. doi: 10.3390/ijms21249681
- Zhang X, Powell K, Li L.** Breast Cancer Stem Cells: Biomarkers, Identification and Isolation Methods, Regulating Mechanisms, Cellular Origin, and Beyond. *Cancers (Basel)*. 2020;12(12):3765. doi: 10.3390/cancers12123765
- Adekola K, Rosen ST, Shanmugam M.** Glucose transporters in cancer metabolism. *Curr Opin Oncol*. 2012;24(6):650-654. doi: 10.1097/CCO.0b013e328356da72
- Lu H, Forbes RA, Verma A.** Hypoxia-inducible factor 1 activation by aerobic glycolysis implicates the Warburg effect in carcinogenesis. *J Biol Chem*. 2002;277(26):23111-23115. doi: 10.1074/jbc.M202487200
- Palomeras S, Ruiz-Martínez S, Puig T.** Targeting Breast Cancer Stem Cells to Overcome Treatment Resistance. *Molecules*. 2018;23(9). doi: 10.3390/molecules23092193
- Nauck MA.** Update on developments with SGLT2 inhibitors in the management of type 2 diabetes. *Drug Des Devel Ther*. 2014;8:1335-1380. doi: 10.2147/dddt.s50773
- Sabaa M, Sharawy MH, El-Sherbiny M, Said E, Salem HA, Ibrahim TM.** Canagliflozin interrupts mTOR-mediated inflammatory signaling and attenuates DMBA-induced mammary cell carcinoma in rats. *Biomed Pharmacother*. 2022;155:113675. doi: 10.1016/j.biopha.2022.113675
- Alimova IN, Liu B, Fan Z, Edgerton SM, Dillon T, Lind SE, et al.** Metformin inhibits breast cancer cell growth, colony

- formation and induces cell cycle arrest in vitro. *Cell Cycle*. 2009;8(6):909-915. doi: 10.4161/cc.8.6.7933
11. **Guo Z, Zhao M, Howard EW, Zhao Q, Parris AB, Ma Z, et al.** Phenformin inhibits growth and epithelial-mesenchymal transition of ErbB2-overexpressing breast cancer cells through targeting the IGF1R pathway. *Oncotarget*. 2017;8(36):60342-60357. doi: 10.18632/oncotarget.19466
  12. **Alhoshani A, Alotaibi M, As Sobeai HM, Alharbi N, Alhazzani K, Al-Dhfyhan A, et al.** In vivo and in vitro studies evaluating the chemopreventive effect of metformin on the aryl hydrocarbon receptor-mediated breast carcinogenesis. *Saudi J Biol Sci*. 2021;28(12):7396-7403. doi: 10.1016/j.sjbs.2021.08.051
  13. **Zhang Y, Xu B, Zhang XP.** Effects of miRNAs on functions of breast cancer stem cells and treatment of breast cancer. *Onco Targets Ther*. 2018;11:4263-4270. doi: 10.2147/ott.s165156
  14. **Li WJ, Wang Y, Liu R, Kasinski AL, Shen H, Slack FJ, et al.** MicroRNA-34a: Potent Tumor Suppressor, Cancer Stem Cell Inhibitor, and Potential Anticancer Therapeutic. *Front Cell Dev Biol*. 2021;9:640587. doi: 10.3389/fcell.2021.640587
  15. **Liu C, Rokavec M, Huang Z, Hermeking H.** Salicylate induces AMPK and inhibits c-MYC to activate a NRF2/ARE/miR-34a/b/c cascade resulting in suppression of colorectal cancer metastasis. *Cell Death Dis*. 2023;14(10):707. doi: 10.1038/s41419-023-06226-9
  16. **Deng X, Zheng H, Li D, Xue Y, Wang Q, Yan S, et al.** MicroRNA-34a regulates proliferation and apoptosis of gastric cancer cells by targeting silent information regulator 1. *Exp Ther Med*. 2018;15(4):3705-3714. doi: 10.3892/etm.2018.5920
  17. **Zhang C, Mo R, Yin B, Zhou L, Liu Y, Fan J.** Tumor suppressor microRNA-34a inhibits cell proliferation by targeting Notch1 in renal cell carcinoma. *Oncol Lett*. 2014;7(5):1689-1694. doi: 10.3892/ol.2014.1931
  18. **National Research Council (US).** Guide for the Care and Use of Laboratory Animals. 8<sup>th</sup> ed. Washington (DC): National Academies Press (US); 2011.
  19. **Kinoshita Y, Yoshioka M, Emoto Y, Yuri T, Yuki M, Koyama C, et al.** Dietary effect of mead acid on DMBA-induced breast cancer in female Sprague-Dawley rats. *Int J Funct Nutr*. 2020;1(2):7. doi: 10.3892/ijfn.2020.7
  20. **Faustino-Rocha A, Oliveira PA, Pinho-Oliveira J, Teixeira-Guedes C, Soares-Maia R, da Costa RG, et al.** Estimation of rat mammary tumor volume using caliper and ultrasonography measurements. *Lab Anim (NY)*. 2013;42(6):217-224. doi: 10.1038/labam.254
  21. **Al Za'abi M, Ali BH, Al Suleimani Y, Adham SA, Ali H, Manoj P, et al.** The Effect of Metformin in Diabetic and Non-Diabetic Rats with Experimentally-Induced Chronic Kidney Disease. *Biomolecules*. 2021;11(6):814. doi: 10.3390/biom11060814

22. **Durak A, Olgar Y, Degirmenci S, Akkus E, Tuncay E, Turan B.** A SGLT2 inhibitor dapagliflozin suppresses prolonged ventricular-repolarization through augmentation of mitochondrial function in insulin-resistant metabolic syndrome rats. *Cardiovasc Diabetol.* 2018;17(1):144. doi: 10.1186/s12933-018-0790-0
23. **Tietz NW, Cook T, McNiven MA.** *Clinical Guide to Laboratory Tests.* W.B. Saunders, Co.: Philadelphia; 1995.
24. **Lowry OH, Rosebrough NJ, Farr AL, Randall RJ.** Protein measurement with the Folin phenol reagent. *J Biol Chem.* 1951;193(1):265-275.
25. **Yesildag K, Gur C, Ileriturk M, Kandemir FM.** Evaluation of oxidative stress, inflammation, apoptosis, oxidative DNA damage and metalloproteinases in the lungs of rats treated with cadmium and carvedilol. *Mol Biol Rep.* 2022;49(2):1201-1211. doi: 10.1007/s11033-021-06948-z
26. **Pereira F, Rosenmann E, Nylen E, Kaufman M, Pinsky L, Wrogemann K.** The 56 kDa androgen binding protein is an aldehyde dehydrogenase. *Biochem Biophys Res Commun.* 1991;175(3):831-838. doi: 10.1016/0006-291x(91)91640-x
27. **Morsy SAA, Fathelbab MH, El-Sayed NS, El-Habashy SE, Aly RG, Harby SA.** Doxycycline-Loaded Calcium Phosphate Nanoparticles with a Pectin Coat Can Ameliorate Lipopolysaccharide-Induced Neuroinflammation Via Enhancing AMPK. *J Neuroimmune Pharmacol.* 2024;19(1):2. doi: 10.1007/s11481-024-10099-w
28. **Ohkawa H, Ohishi N, Yagi K.** Assay for lipid peroxides in animal tissues by thiobarbituric acid reaction. *Anal Biochem.* 1979;95(2):351-358. doi: 10.1016/0003-2697(79)90738-3
29. **Nishikimi M, Appaji N, Yagi K.** The occurrence of superoxide anion in the reaction of reduced phenazine methosulfate and molecular oxygen. *Biochem Biophys Res Commun.* 1972;46(2):849-854. doi: 10.1016/s0006-291x(72)80218-3
30. **Rao X, Huang X, Zhou Z, Lin X.** An improvement of the  $2^{-\Delta\Delta CT}$  method for quantitative real-time polymerase chain reaction data analysis. *Biostat Bioinforma Biomath.* 2013;3(3):71-85.
31. **Zhang X, Bao C, Zhang J.** Inotodiol suppresses proliferation of breast cancer in rat model of type 2 diabetes mellitus via downregulation of  $\beta$ -catenin signaling. *Biomed Pharmacother.* 2018;99:142-150. doi: 10.1016/j.biopha.2017.12.084
32. **Zhang X, Powell K, Li L.** Breast Cancer Stem Cells: Biomarkers, Identification and Isolation Methods, Regulating Mechanisms, Cellular Origin, and Beyond. *Cancers (Basel).* 2020;12(12). doi: 10.3390/cancers12123765
33. **Ganapathy V, Thangaraju M, Prasad PD.** Nutrient transporters in cancer: relevance to Warburg hypothesis and beyond. *Pharmacol Ther.* 2009;121(1):29-40. doi: 10.1016/j.pharmthera.2008.09.005
34. **Thompson HJ, Singh M.** Rat models of premalignant breast disease. *J Mammary*

- Gland Biol Neoplasia. 2000;5(4):409-420. doi: 10.1023/a:1009582012493
35. **Russo J, Russo IH.** Experimentally induced mammary tumors in rats. *Breast Cancer Res Treat.* 1996;39(1):7-20. doi: 10.1007/bf01806074
36. **Alvarado A, Faustino-Rocha AI, Colaço B, Oliveira PA.** Experimental mammary carcinogenesis - Rat models. *Life Sci.* 2017;173:116-134. doi: 10.1016/j.lfs.2017.02.004
37. **Setiawan T, Sari IN, Wijaya YT, Julianto NM, Muhammad JA, Lee H, et al.** Cancer cachexia: molecular mechanisms and treatment strategies. *J Hematol Oncol.* 2023;16(1):54. doi: 10.1186/s13045-023-01454-0
38. **Wang Z, Zhang X.** Chemopreventive Activity of Honokiol against 7, 12 - Dimethylbenz[a]anthracene-Induced Mammary Cancer in Female Sprague Dawley Rats. *Front Pharmacol.* 2017;8:320. doi: 10.3389/fphar.2017.00320
39. **Karnam KC, Ellutla M, Bodduluru LN, Kasala ER, Uppulapu SK, Kalyankumarraju M, et al.** Preventive effect of berberine against DMBA-induced breast cancer in female Sprague Dawley rats. *Biomed Pharmacother.* 2017;92:207-214. doi: 10.1016/j.biopha.2017.05.069
40. **Krishnamoorthy D, Sankaran M.** Modulatory effect of *Pleurotus ostreatus* on oxidant/antioxidant status in 7, 12-dimethylbenz (a) anthracene induced mammary carcinoma in experimental rats-- A dose-response study. *J Cancer Res Ther.* 2016;12(1):386-394. doi: 10.4103/0973-1482.148691
41. **Akhouri V, Kumari M, Kumar A.** Therapeutic effect of *Aegle marmelos* fruit extract against DMBA induced breast cancer in rats. *Sci Rep.* 2020;10(1):18016. doi: 10.1038/s41598-020-72935-2
42. **Glaviano A, Foo ASC, Lam HY, Yap KCH, Jacot W, Jones RH, et al.** PI3K/AKT/mTOR signaling transduction pathway and targeted therapies in cancer. *Mol Cancer.* 2023;22(1):138. doi: 10.1186/s12943-023-01827-6
43. **Fan H, Wu Y, Yu S, Li X, Wang A, Wang S, et al.** Critical role of mTOR in regulating aerobic glycolysis in carcinogenesis (Review). *Int J Oncol.* 2021;58(1):9-19. doi: 10.3892/ijo.2020.5152
44. **Shiau JP, Chuang YT, Cheng YB, Tang JY, Hou MF, Yen CY, et al.** Impacts of Oxidative Stress and PI3K/AKT/mTOR on Metabolism and the Future Direction of Investigating Fucoidan-Modulated Metabolism. *Antioxidants.* 2022;11(5):911. doi: 10.3390/antiox11050911
45. **Ouhtit A, Ismail MF, Othman A, Fernando A, Abdraboh ME, El-Kott AF, et al.** Chemoprevention of rat mammary carcinogenesis by spirulina. *Am J Pathol.* 2014;184(1):296-303. doi: 10.1016/j.ajpath.2013.10.025
46. **Elledge RM, Allred DC.** The p53 tumor suppressor gene in breast cancer. *Breast Cancer Res Treat.* 1994;32(1):39-47. doi: 10.1007/bf00666204

47. **Marvalim C, Datta A, Lee SC.** Role of p53 in breast cancer progression: An insight into p53 targeted therapy. *Theranostics*. 2023;13(4):1421-1442. doi: 10.7150/thno.81847
48. **Nishimura J, Dewa Y, Muguruma M, Kuroiwa Y, Yasuno H, Shima T, et al.** Effect of fenofibrate on oxidative DNA damage and on gene expression related to cell proliferation and apoptosis in rats. *Toxicol Sci*. 2007;97(1):44-54. doi: 10.1093/toxsci/kfm011
49. **Shetzer Y, Molchadsky A, Rotter V.** Oncogenic Mutant p53 Gain of Function Nourishes the Vicious Cycle of Tumor Development and Cancer Stem-Cell Formation. *Cold Spring Harb Perspect Med*. 2016;6(10). doi: 10.1101/cshperspect.a026203
50. **Lee CW, Wong LL, Tse EY, Liu HF, Leong VY, Lee JM, et al.** AMPK promotes p53 acetylation via phosphorylation and inactivation of SIRT1 in liver cancer cells. *Cancer Res*. 2012;72(17):4394-4404. doi: 10.1158/0008-5472.can-12-0429
51. **Keerthana CK, Rayginia TP, Shifana SC, Anto NP, Kalimuthu K, Isakov N, et al.** The role of AMPK in cancer metabolism and its impact on the immunomodulation of the tumor microenvironment. *Front Immunol*. 2023;14:1114582. doi: 10.3389/fimmu.2023.1114582
52. **Ghanbari Movahed Z, Rastegari-Pouyani M, Mohammadi MH, Mansouri K.** Cancer cells change their glucose metabolism to overcome increased ROS: One step from cancer cell to cancer stem cell? *Biomed Pharmacother*. 2019;112:108690. doi: 10.1016/j.biopha.2019.108690
53. **Koppenol WH, Bounds PL, Dang CV.** Otto Warburg's contributions to current concepts of cancer metabolism. *Nat Rev Cancer*. 2011;11(5):325-337. doi: 10.1038/nrc3038
54. **Lunt SY, Vander Heiden MG.** Aerobic glycolysis: meeting the metabolic requirements of cell proliferation. *Annu Rev Cell Dev Biol*. 2011;27:441-464. doi: 10.1146/annurev-cellbio-092910-154237
55. **Evens JM, Donnelly LA, Emslie-Smith AM, Alessi DR, Morris AD.** Metformin and reduced risk of cancer in diabetic patients. *Bmj*. 2005;330(7503):1304-1305. doi: 10.1136/bmj.38415.708634.F7
56. **Shi B, Hu X, He H, Fang W.** Metformin suppresses breast cancer growth via inhibition of cyclooxygenase-2. *Oncol Lett*. 2021;22(2):615. doi: 10.3892/ol.2021.12876
57. **Karim S, Alghanmi AN, Jamal M, Alkreathy H, Jamal A, Alkhatabi HA, et al.** A comparative in vitro study on the effect of SGLT2 inhibitors on chemosensitivity to doxorubicin in MCF-7 breast cancer cells. *Oncol Res*. 2024;32(5):817-830. doi: 10.32604/or.2024.048988
58. **Zhou J, Zhu J, Yu SJ, Ma HL, Chen J, Ding XF, et al.** Sodium-glucose co-transporter-2 (SGLT-2) inhibition reduces glucose uptake to induce breast cancer cell growth arrest through AMPK/mTOR

- pathway. *Biomed Pharmacother.* 2020;132:110821. doi: 10.1016/j.biopha.2020.110821
59. **Wright EM. SGLT2 and cancer.** *Pflugers Arch.* 2020;472(9):1407-1414. doi: 10.1007/s00424-020-02448-4
60. **Dutka M, Bobiński R, Francuz T, Garczorz W, Zimmer K, Ilczak T, et al.** SGLT-2 Inhibitors in Cancer Treatment-Mechanisms of Action and Emerging New Perspectives. *Cancers (Basel).* 2022;14(23):5811. doi: 10.3390/cancers14235811
61. **Barbosa AM, Martel F.** Targeting Glucose Transporters for Breast Cancer Therapy: The Effect of Natural and Synthetic Compounds. *Cancers (Basel).* 2020;12(1):154. doi: 10.3390/cancers12010154
62. **Hung MH, Chen YL, Chen LJ, Chu PY, Hsieh FS, Tsai MH, et al.** Canagliflozin inhibits growth of hepatocellular carcinoma via blocking glucose-influx-induced  $\beta$ -catenin activation. *Cell Death Dis.* 2019;10(6):420. doi: 10.1038/s41419-019-1646-6
63. **Yip JMX, Chiang GSH, Lee ICJ, Lehming-Teo R, Dai K, Dongol L, et al.** Mitochondria and the Repurposing of Diabetes Drugs for Off-Label Health Benefits. *Int J Mol Sci.* 2025;26(1):364. doi: 10.3390/ijms26010364
64. **Ma T, Tian X, Zhang B, Li M, Wang Y, Yang C, et al.** Low-dose metformin targets the lysosomal AMPK pathway through PEN2. *Nature.* 2022;603(7899):159-165. doi: 10.1038/s41586-022-04431-8
65. **Foretz M, Guigas B, Viollet B.** Understanding the glucoregulatory mechanisms of metformin in type 2 diabetes mellitus. *Nat Rev Endocrinol.* 2019;15(10):569-589. doi: 10.1038/s41574-019-0242-2
66. **Tsai KL, Hsieh PL, Chou WC, Cheng HC, Huang YT, Chan SH.** Dapagliflozin attenuates hypoxia/reoxygenation-caused cardiac dysfunction and oxidative damage through modulation of AMPK. *Cell Biosci.* 2021;11(1):44. doi: 10.1186/s13578-021-00547-y
67. **Katsuumi G, Shimizu I, Suda M, Yoshida Y, Furihata T, Joki Y, et al.** SGLT2 inhibition eliminates senescent cells and alleviates pathological aging. *Nat Aging.* 2024;4(7):926-938. doi: 10.1038/s43587-024-00642-y
68. **Jones RG, Plas DR, Kubek S, Buzzai M, Mu J, Xu Y, et al.** AMP-activated protein kinase induces a p53-dependent metabolic checkpoint. *Mol Cell.* 2005;18(3):283-293. doi: 10.1016/j.molcel.2005.03.027
69. **Yao S, Gao M, Wang Z, Wang W, Zhan L, Wei B.** Upregulation of MicroRNA-34a Sensitizes Ovarian Cancer Cells to Resveratrol by Targeting Bcl-2. *Yonsei Med J.* 2021;62(8):691-701. doi: 10.3349/ymj.2021.62.8.691
70. **Li WJ, Liu X, Dougherty EM, Tang DG.** MicroRNA-34a, Prostate Cancer Stem Cells, and Therapeutic Development. *Cancers (Basel).* 2022;14(18):4538. doi: 10.3390/cancers14184538
71. **Imani S, Wei C, Cheng J, Khan MA, Fu S, Yang L, et al.** MicroRNA-34a targets

- epithelial to mesenchymal transition-inducing transcription factors (EMT-TFs) and inhibits breast cancer cell migration and invasion. *Oncotarget*. 2017;8(13):21362-21379. doi: 10.18632/oncotarget.15214
72. **Bommer GT, Gerin I, Feng Y, Kaczorowski AJ, Kuick R, Love RE, et al.** p53-mediated activation of miRNA34 candidate tumor-suppressor genes. *Curr Biol*. 2007;17(15):1298-1307. doi: 10.1016/j.cub.2007.06.068
73. **Villani LA, Smith BK, Marcinko K, Ford RJ, Broadfield LA, Green AE, et al.** The diabetes medication Canagliflozin reduces cancer cell proliferation by inhibiting mitochondrial complex-I supported respiration. *Mol Metab*. 2016;5(10):1048-1056. doi: 10.1016/j.molmet.2016.08.014
74. **Luis G, Godfroid A, Nishiumi S, Cimino J, Blacher S, Maquoi E, et al.** Tumor resistance to ferroptosis driven by Stearoyl-CoA Desaturase-1 (SCD1) in cancer cells and Fatty Acid Binding Protein-4 (FABP4) in tumor microenvironment promote tumor recurrence. *Redox Biol*. 2021;43:102006. doi: 10.1016/j.redox.2021.102006
75. **Eliaa SG, Al-Karmalawy AA, Saleh RM, Elshal MF.** Empagliflozin and Doxorubicin Synergistically Inhibit the Survival of Triple-Negative Breast Cancer Cells via Interfering with the mTOR Pathway and Inhibition of Calmodulin: In Vitro and Molecular Docking Studies. *ACS Pharmacol Transl Sci*. 2020;3(6):1330-1338. doi: 10.1021/acsptsci.0c00144
76. **Naeimzadeh Y, Tajbakhsh A, Nemati M, Fallahi J.** Exploring the anti-cancer potential of SGLT2 inhibitors in breast cancer treatment in pre-clinical and clinical studies. *Eur J Pharmacol*. 2024;978:176803. doi: 10.1016/j.ejphar.2024.176803